

Frequently Methylated Tumor Suppressor Genes in Head and Neck Squamous Cell Carcinoma

Kristi L. Bennett,^{1,4} Matthew Karpenko,² Mau-ting Lin,^{3,4} Rainer Claus,^{4,5} Khelifa Arab,⁵ Gerhard Dyckhoff,⁶ Peter Plinkert,⁶ Esther Herpel,⁷ Dominic Smiraglia,⁸ and Christoph Plass^{1,4,5}

¹Department of Molecular Genetics, The Ohio State University; ²Department of Internal Medicine, Division of Hematology/Oncology, The Ohio State University Medical Center; ³Molecular, Cellular, and Developmental Biology Graduate Program; ⁴Department of Molecular Virology, Immunology, and Medical Genetics, Division of Human Cancer Genetics, The Comprehensive Cancer Center, The Ohio State University, Columbus, Ohio; ⁵Division of Toxicology and Cancer Risk Factors, German Cancer Research Center; Departments of ⁶Head and Neck Surgery and ⁷General Pathology, University of Heidelberg, Heidelberg, Germany; and ⁸Department of Cancer Genetics, Roswell Park Cancer Institute, Buffalo, New York

Abstract

Head and neck squamous cell carcinoma (HNSCC) is a very aggressive cancer. In advanced stages, the patient has poor chances of receiving effective treatment, and survival rates are low. To facilitate timely diagnosis and improve treatment, elucidation of early detection markers is crucial. DNA methylation markers are particularly advantageous because DNA methylation is an early event in tumorigenesis, and the epigenetic modification, 5-methylcytosine, is a stable mark. A genome-wide screen using Restriction Landmark Genomic Scanning found a set of genes that are most commonly methylated in head and neck cancers. Five candidate genes: *septin 9* (*SEPT9*), *sodium-coupled monocarboxylate transporter 1* (*SLC5A8*), *functional smad-suppressing element on chromosome 18* (*FUSSEL18*), *early B-cell factor 3* (*EBF3*), and *iroquois homeobox 1* (*IRX1*) were methylated in 27% to 67% of the HNSCC patient samples tested. Furthermore, ~50% of the methylated tumor samples shared methylation between two of the five genes (most commonly between *EBF3* and *IRX1*), and 15% shared methylation between three of the five genes. Expression analysis revealed candidate gene down-regulation in 25% to 93% of the HNSCC samples, and 5-aza-2'-deoxycytidine treatment was able to restore expression in at least 2 of 5 HNSCC cell lines for all of the genes tested. Overexpression of the three most frequently down-regulated candidates, *SLC5A8*, *IRX1*, and *EBF3*, validated their tumor suppressor potential by growth curve analysis and colony formation assay. Interestingly, all of the candidates identified may be involved in the transforming growth factor β signaling pathway, which is often disrupted in HNSCC. [Cancer Res 2008;68(12):4494-9]

Introduction

Head and neck squamous cell carcinoma (HNSCC) is the sixth most common cancer worldwide. According to the National Cancer Institute's Surveillance Epidemiology and End Results cancer statistics review, 34,360 individuals were predicted to be diagnosed with HNSCC in 2007. Treatment of HNSCC is complex,

using radiation therapy, surgery, and chemoradiation. Patients with advanced HNSCC are limited to a complete response of 50% and often require long-term rehabilitation. However, early HNSCC detection increases survival to 80%. Therefore, early detection markers may potentially serve as a predictive tool for diagnosis and recurrence of HNSCC (1).

DNA methylation within the promoter region of a gene can result in chromatin compaction and inhibition or down-regulation of gene transcription. Aberrant promoter methylation is often responsible for gene silencing in a variety of malignancies, and several genes have been shown to be epigenetically down-regulated in HNSCC (2). Because methylation is an early event, identification of methylation markers could provide great promise for early detection and treatment in HNSCC (1).

Our laboratory uses a technique called Restriction Landmark Genomic Scanning (RLGS) for genome-wide promoter methylation analysis. Previous RLGS analysis on several HNSCC patient samples revealed more methylation in metastatic HNSCC samples compared with primary tumors, and the methylated loci in metastatic versus primary tumors within the same patient were found to be dissimilar (3). Also, RLGS analysis has been used to identify amplification of potential oncogenes in HNSCC (4). The study described here used these RLGS profiles to identify potential novel tumor suppressor genes that are frequently methylated in HNSCC. This analysis provided 5 genes (*IRX1*, *FUSSEL18*, *EBF3*, *SLC5A8*, and *SEPT9*) that were epigenetically silenced in >10% of the patient samples analyzed. Interestingly, these genes have previously been found to exhibit tumor suppressor activity in cancer (5-9). Also, they have been shown to potentially be involved in transforming growth factor (TGF- β) signaling (5, 10-13), which is often disrupted in HNSCC (14-16).

Materials and Methods

Patient samples and cell lines. Frozen tumor tissues and adjacent normal mucosa tissue (normals) from HNSCC patients were attained from The Ohio State University Medical Center via the Cooperative Human Tissue Network. Surgery was performed on all patients at The Ohio State University Medical Center. Control samples were collected from morphologically normal tissue located at least 3 cm from the tumor margin. Histopathologic evaluation was performed on all samples for verification. A second set of HNSCC and normal mucosa was obtained from the Tissuebank of the National Center of Tumor Diseases, Heidelberg. All sample collections were done according to the NIH guidelines and under a protocol approved by The Ohio State University's or the Medical Faculty Heidelberg's Institutional Review Boards. The five different established human HNSCC cell lines used in the study (SCC8, SCC11B, SCC17AS, SCC22B, and SCC25) were kindly provided by Dr. Thomas Carey (University

Note: Supplementary data for this article are available at Cancer Research Online (<http://cancerres.aacrjournals.org/>).

Requests for reprints: Christoph Plass, German Cancer Research Center (DKFZ), Division C010, Toxicology and Cancer Risk Factors, Im Neuenheimer Feld 280, 69120 Heidelberg, Germany. Phone: 49-6221-42-3300; Fax: 49-6221-42-3359; E-mail: c.plass@dkfz.de.

©2008 American Association for Cancer Research.
doi:10.1158/0008-5472.CAN-07-6509

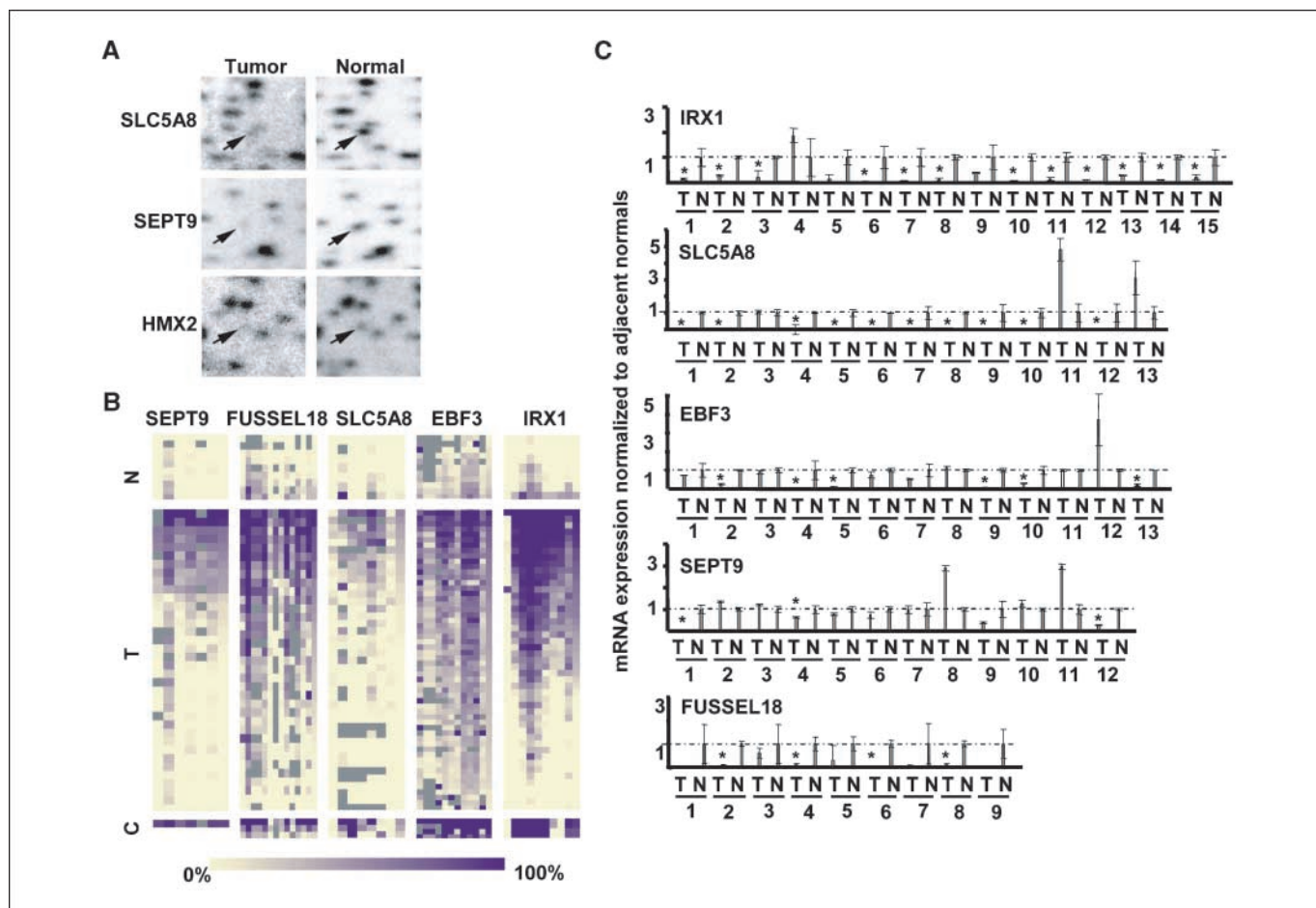


Figure 1. Methylation and expression of candidate genes in HNSCC. *A*, examples of decreased intensity fragments identified by RFLG analysis. Three loci are shown as examples (HMX2, SEPT9, and SLC5A8). The profiles on the right are generated from adjacent normal tissue, whereas the profiles on the left come from HNSCC tumor tissue. *Arrows*, fragment of interest. Decreased intensity is assessed by comparing with the profile of its adjacent normal. *B*, MassARRAY broad methylation analysis. The heat maps display the different genes tested for methylation. Each row represents a different sample, each column represents a CpG site or group of CpGs. The top section represents normals (*N*), the middle section consists of tumor samples (*T*), and the bottom section is HNSCC cell lines (*C*). Increasing color intensity represents increasing methylation. *C*, relative candidate mRNA expression in HNSCC tumors. The five candidates from the methylation summary were subjected to quantitative RT-PCR analysis. Each bar represents the expression of HNSCC tumor or adjacent normal. The tumor expression is normalized to its matched adjacent normal, which is set to a value of 1 (*dashed line*). Samples in which the expression level in the tumor is significantly ($P < 0.05$) reduced are marked (*).

of Michigan, Ann Arbor, MI). Cell lines were maintained in DMEM with 10% fetal bovine serum and 1% streptomycin/penicillin antibiotics.

MassARRAY methylation analysis. Quantitative DNA methylation analysis was performed by MassARRAY technique. Briefly, 1 μ g of HNSCC patient or cell line DNA was bisulfite treated, *in vitro* transcribed, cleaved by RNase A, and subjected to MALDI-TOF mass spectrometry analysis to determine methylation patterns, as previously described (17). To normalize for any bias, standards (0%, 5%, 10%, 20%, 40%, 60%, 80%, and 100% *Sss*I methylated) were included in the assay to generate an "observed to expected plot." The equation of the best-fitting line was then used to normalize the values for the HNSCC samples. Subsequent to normalization, tumor samples with more methylation than adjacent normal samples were considered methylated. The methylation results are displayed as a heat map using the Mutiple Experimental Viewer software (18).

RNA isolation and cDNA synthesis. RNA was isolated according to the manufacturer's protocol. DNase treatment was performed on 1 to 2 μ g of RNA by adding 2 U of DNaseI (Invitrogen), 1 μ L DNase buffer, and 0.4 μ L RNase Out (Invitrogen) for 15 min at room temperature. One microliter of EDTA was then added to the mix for 10 min at 65°C, followed by an incubation on ice for 5 min. Complementary DNA synthesis was performed by the following reaction: 2 μ L random hexamers and 1 μ L deoxynucleotide triphosphates (10 mmol/L) for 5 min at 65°C, then 2 min at 4°C; 2 μ L of

10 \times buffer, 4 μ L MgCl₂, 2 μ L DTT, and 1 μ L RNase Out was added for 2 min at 25°C; 100 U of SuperScript II (Invitrogen) for 50 min at 42°C; 15 min at 70°C, then transferred to 4°C.

5-aza-2'-deoxycytidine treatment. HNSCC cell lines were incubated for 96 h with 1 μ mol/L 5-aza-2'-deoxycytidine (5-aza-dC; Sigma) with medium changed every day. Treated cells were harvested for analysis 1 to 4 d after the procedure. Cells were suspended in Trizol for RNA isolation.

Real-time PCR. Quantitative mRNA expression was measured using SYBR Green I (Bio-Rad) in an I-Cycler (Bio-Rad). Expression of glycosylphosphatidylinositol was used as the internal control gene. I-Cycler conditions and real-time PCR (RT-PCR) primers can be provided upon request. For the RT-PCRs on the HNSCC patient samples, each tumor was normalized to the expression of its adjacent normal tissue, which was set to a value of 1. For the 5-aza-dC-treated HNSCC cell lines, each treated cell line was normalized to its untreated counterpart, which was set to a value of 1.

Plasmids. The SLC5A8 overexpression vector was provided by Dr. Joe Costello (University of California, San Francisco, CA). The 1.71-kb EBF3 cDNA was cloned into the *Eco*RI site of pBABE, and the 1.61-kb IRX1 cDNA was cloned into the *Bam*HI and *Sal*I sites of pBABE.

Transfections. Stable transfections were performed as previously described (19). Briefly, 120 h postinfection, the target cells were collected,

Table 1. Complete summary of RLGS analysis in HNSCC

Fragment	Chrom	Gene	Freq	1	2	3	4	5	6	7	8	9	10	11	12	13	14	15	16	17	18	19	20	21	22
4E06			19	■	■				■	■	■	■	■			■	■	■	■	■	■	■	■	■	■
2B55			18	■	■			■	■	■	■	■	■			■	■	■	■	■	■	■	■	■	■
2E33	1p13.3	ALX3	0						NA						■			■			■	■	■	■	■
2D64			11							■	■	■	■				■					■	■	■	■
3F82	16p11.2		9	NA				NA	NA				■	■							■	■	■	■	■
4D08	17q25.3	SEPT9	9					■		■	■	■	■								■	■	■	■	■
3D57	10q26.13	HMX2	8	■	■			■		■	■	■	■									■	■	■	■
3D41	12q23.2	SLC5A8	7							■	■	■	■									■	■	■	■
3E25	16q12.1		8				■					■	■								■	■	■	■	■
2E64	12q24.21		6				■			■	■	■	■									■	■	■	■
3F61			6	■							■	■	■				■					■	■	■	■
3C02	5p15.33	IRX1	5							■	■	■	■					■					■	■	■
3E54			5							■	■	■	■										■	■	■
3F19			6	■					■		■	■	■			■	■					■	■	■	■
3F28			5		■							■	■										■	■	■
4E33			5							■	■	■	■										■	■	■
5B31			5				■					■	■										■	■	■
2E30	18q21.1	FUSSEL18	4							■	■	■	■											■	■
2B54	10q26.3	EBF3	4									■	■											■	■
3C21			5							■	■	■	■											■	■
3D03			4							■	■	■	■											■	■
3E36			4	■								■	■								■	■	■	■	■
3F10	2q37.2	GBX2	4									■	■				■							■	■

NOTE: The table shows the different RLGS fragments lost in at least 10% (4 of 42) of the profiles. Chromosomal locations are provided for the cloned fragments, as well as any associated genes. *Freq*, the number of profiles in which that fragment displayed decreased intensity compared with normal. All patient profiles are listed, 1 through 42, to show shared methylation events within a given patient. *NA*, fragment was unanalyzable for that patient sample, most likely because of background.

RNA isolated, and cDNA synthesized for RT-PCR confirmation of over-expression.

Growth curve. Five thousand cells were plated in triplicates in a 6-well plate for a 5-d growth curve analysis. For each count, 500 μ L of trypsin was added to each well for 3 min, after which the cells were suspended in 2 mL of PBS, and 500 μ L was counted using a Coulter counter.

Colony formation assay. One thousand cells were plated in triplicates in 60-cm plates. After 10 d, the medium were removed and the cells were washed with PBS and fixed with 2:1 methanol:acetic acid for 15 min. Staining was performed using 0.1% crystal violet PBS for 30 min shaking at room temperature. Stain was removed, cells were washed with water, and colonies were counted.

Statistical analysis. The statistical significance of the results was calculated by unpaired Student's *t* test, and $P < 0.05$ was considered to be statistically significant.

Results

RLGS analysis in HNSCC patient samples. Global methylation analysis via RLGS has previously been performed on 42 HNSCC patient samples (3, 4). However, these critiques only focused on general changes in methylation between primary and metastatic tumors and demethylation of potential oncogenes. Therefore, these profiles were reevaluated to identify the specific genes (potential tumor suppressors) that are frequently methylated in HNSCC. This analysis yielded 23 different loci among the profiles that had decreased RLGS fragment intensity in >10% of the profiles [examples shown in Fig. 1A and complete list in Table 1; the 10% cutoff provides a significant difference ($P < 0.05$)]. Eleven of these

fragments have been previously cloned, eight of which were found to be associated with a CpG island and a known gene: *ALX3*, *HMX2*, *SLC5A8*, *SEPT9*, *FUSSEL18*, *EBF3*, *IRX1*, and *GBX2* (Table 1). BLAT analysis revealed that 7 of 8 of these genes had CpG islands upstream of their transcription start sites, and *SEPT9* contained several within the transcribed region. This analysis revealed that 69% (29 of 42) of the HNSCC patients had at least one of these 8 genes methylated. Of these, 31% (9 of 29) had shared methylation between 2 genes, and 14% (4 of 29) had shared methylation between 4 or 6 genes (Table 1).

Confirmation of DNA methylation by high-throughput MassARRAY DNA methylation analysis. The MassARRAY technique was used to attain a broad and quantitative DNA methylation analysis of the gene promoters. Primers were designed near or upstream of the transcription start site and/or within the associated CpG island. The genes found to be methylated by a preliminary methylation screen were selected for the MassARRAY (i.e., *SEPT9*, *FUSSEL18*, *SLC5A8*, *EBF3*, and *IRX1*). The MassARRAY analysis revealed 56% (20 of 36) of the tumor samples with *SEPT9* methylation, 49% (17 of 35) with methylation for *FUSSEL18*, 32% (13 of 41) *SLC5A8* methylation, 50% (28 of 56) *EBF3* methylation in tumors, and 45% (21 of 47) showed *IRX1* methylation (Fig. 1B). These data were further validated in a separate set of 20 HNSCC samples and 18 samples of normal mucosa (Supplementary Fig. S1). Of the tumor samples found to be methylated by the MassARRAY analysis, >50% were methylated in at least 2 of the candidate genes. Also,

possibility for using comethylation for improved diagnosis but also suggests that the candidates described in this study may be involved in a similar pathway that is disrupted and epigenetically silenced in HNSCC. TGF- β signaling has been found to be disrupted in HNSCC progression; therefore, this pathway has been targeted for therapy (14). Aberrant expression of hypoxia-induced proteins has also been shown to have relevance for HNSCC progression and prognosis prediction (15). Furthermore, evidence supports the synergistic cooperation between the hypoxia and TGF- β signaling pathways (16). Interestingly, the candidates elucidated in our study may be involved in these pathways (Supplementary Fig. S2). FUSSEL18 has been shown to bind Smad

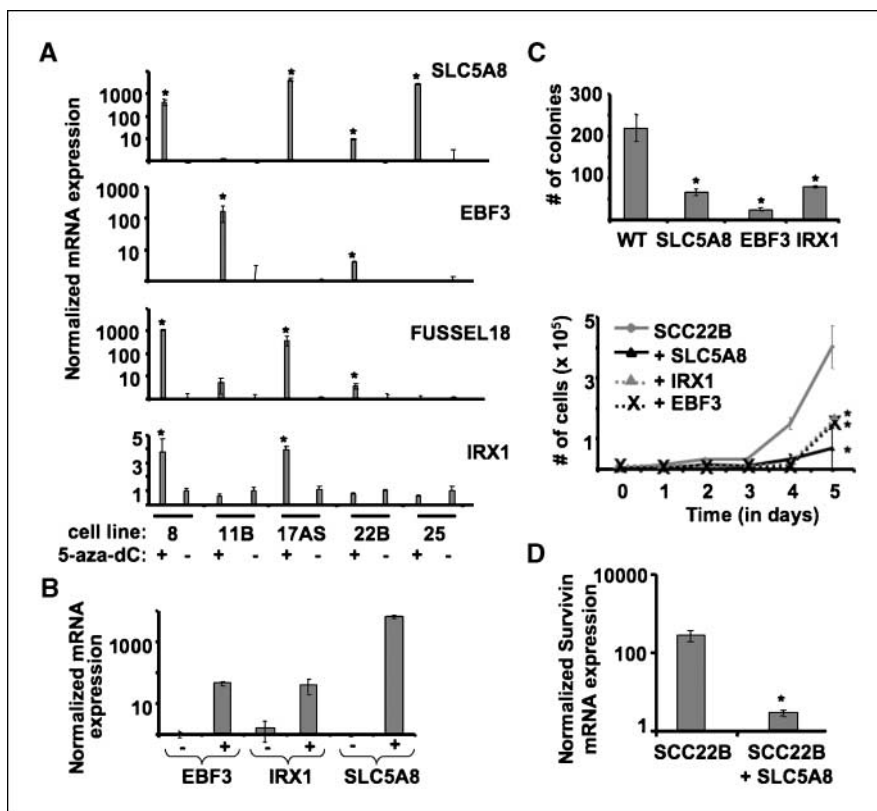
2 and 3 and inhibit TGF- β signaling (11). Also, SEPT9 interacts with HIF-1 α to prevent its ubiquitination and degradation, which can allow TGF- β feedback activation (10). IRX-1 is a downstream target of Smad 2-mediated transcriptional activation (12), and SLC5A8 down-regulates SURVIVIN (target of HIF-1 α) to induce apoptosis (5). EBF3 has been shown to activate p21 (which is a target of HIF-1 α and Smad3), and an EBF-associated zinc-finger protein has been found to bind with Smad proteins (13). Therefore, epigenetic down-regulation of these candidate genes may be critical to disrupt their roles in TGF- β signaling, allowing uncontrolled proliferation and apoptosis resistance for HNSCC progression.

Table 2. Summary of methylated tumor samples from MassARRAY analysis

Tumor	Age	Location	Gender	IRX1	EBF3	SLC5A8	SEPT9	FUSSEL18
1	66	Tongue	M	95			41	
2	51	Oral cavity	M	80	53			
3	56	Tongue	M	76	31			
4	58	Tongue	M	76		50		
5	48	Pharynx	F	76			14	
6	54	Tongue	F	75	62	38		
7	71	Tongue	F	71	32			
8	74	Tongue	M	71	45			
9	4	Tonsil	F	69	33	42		
10	53	Tonsil	M			40	16	
11	80	Oral cavity	F	67	36	41		
12	74	Pharynx	F	65		32		
13	61	Pharynx	M	65	62			
14	52	Pharynx	M	64	40			37
15	57	Oral cavity	M	63	52			
16	60	Pharynx	M	63				
17	64	Pharynx	F	63	42		56	
18	79	Larynx	F	61		26	49	
19	44	Pharynx	M	59		35		
20	64	Larynx	F	57				
21	57	Larynx	M	56				
22	44	Tonsil	F	55	41			
23	49	Tongue	M		69			
24	68	Tonsil	M		52			
25	48	Larynx	F		50			
26	62	Pharynx	M		47			
27	43	Tongue	M		45			
28	46	Pharynx	F		43			
29	68	Oral cavity	F		42			
30	66	Larynx	M		41			
31	58	Oral cavity	F		37	30		
32	70	Oral cavity	M		35			
33	33	Oral cavity	F		34			
34	65	Larynx	M		34			
35	54	Oral cavity	M		34			
36	62	Oral cavity	M		33		25	
37	61	Larynx	M		31			
38	37	Tongue	M		30			
39	78	Larynx	M				43	
40	68	Oral cavity	F					

NOTE: The list contains tumor DNA samples with methylation above that seen in the normal tissue. The numbers below the genes represent percent methylation of that gene for that sample. Additional samples for SLC5A8, SEPT9, and FUSSEL18 are not listed because they were only tested in that gene.

Figure 2. Demethylation increases candidate mRNA expression and candidate gene overexpression provides tumor suppressor activity in HNSCC cell lines. **A**, relative fold increase in candidate mRNA expression in HNSCC cell lines after demethylation treatment. cDNA was synthesized from HNSCC cell lines with and without 1 $\mu\text{mol/L}$ 5-aza-dC for 96 h. Quantitative RT-PCR was performed on the 4 candidates that showed >25% of the samples with decreased mRNA expression in HNSCC tumors compared with normals. Each bar represents the expression of the 5-aza-dC-treated HNSCC cell lines normalized to the untreated HNSCC cell line, which is set to a value of 1. *, $P < 0.050$. **B**, confirmed mRNA overexpression of EBF3, IRX1, and SLC5A8 in an HNSCC cell line SCC22B. cDNA was synthesized from HNSCC cell line SCC22B with and without the overexpression plasmids (EBF3-pBABE, IRX1-pBABE, and SLC5A8-pBABE). Quantitative RT-PCR was performed to validate overexpression. -, wild-type (WT) SCC22B; +, SCC22B infected with that overexpression vector. **C**, decreased colony formation with candidate gene overexpression (top). Colony formation assay was performed with wild-type SCC22B and SCC22B cells overexpressing EBF3, IRX1, and SLC5A8. One thousand cells were plated, and 10 d later, the medium was removed and colonies were stained. The graph represents the number of colonies. *, $P < 0.007$. Bottom, decreased cell numbers with candidate gene overexpression. Growth curve analysis was performed with wild-type SCC22B and SCC22B cells overexpressing EBF3, IRX1, and SLC5A8. Five thousand cells were plated, and each day, the plates were trypsinized and cells counted. *, $P < 0.013$. **D**, decreased Survivin expression in the presence of SLC5A8 overexpression. Quantitative RT-PCR was performed to check Survivin expression. *, $P < 0.015$.



The research discussed in this study may lend the opportunity for improved HNSCC screening and detection. However, more comprehensive studies with large patient sets that incorporate stage and pathology should be performed to confirm whether these markers have prognostic implications. Methylation of the genes described in this study may occur at an early stage, providing great promise for earlier HNSCC detection. Therefore, the methylated candidates revealed in this study deserve further attention to discern their potential worth for HNSCC diagnosis and prognosis prediction.

Disclosure of Potential Conflicts of Interest

No potential conflicts of interest were disclosed.

Acknowledgments

Received 12/7/2007; revised 3/20/2008; accepted 3/21/2008.

Grant support: NIDCR, DE13123 (C. Plass) and an AGGRS scholarship (K. Benett).

The costs of publication of this article were defrayed in part by the payment of page charges. This article must therefore be hereby marked *advertisement* in accordance with 18 U.S.C. Section 1734 solely to indicate this fact.

We thank Dr. Thomas Carey for the HNSCC cell lines (SCC22B, SCC25, SCC8, SCC11B, and SCC17AS) and the members of the Plass Laboratory for thoughtful discussions.

References

1. Goldenberg D, Harden S, Masayeva BG, et al. Intraoperative molecular margin analysis in head and neck cancer. *Arch Otolaryngol Head Neck Surg* 2004;130:39-44.
2. Marsit CJ, McClean MD, Furness CS, et al. Epigenetic inactivation of the SFRP genes is associated with drinking, smoking and HPV in head and neck squamous cell carcinoma. *Int J Cancer* 2006;119:1761-6.
3. Smiraglia DJ, Smith LT, Lang JC, et al. Differential targets of CpG island hypermethylation in primary and metastatic head and neck squamous cell carcinoma (HNSCC). *J Med Genet* 2003;40:25-33.
4. Lin M, Smith LT, Smiraglia DJ, et al. DNA copy number gains in head and neck squamous cell carcinoma. *Oncogene* 2006;25:1424-33.
5. Thangaraju M, Gopal E, Martin PM, et al. SLC5A8 triggers tumor cell apoptosis through pyruvate-dependent inhibition of histone deacetylases. *Cancer Res* 2006;66:11560-4.
6. Zhao LY, Niu Y, Santiago A, et al. An EBF3-mediated transcriptional program that induces cell cycle arrest and apoptosis. *Cancer Res* 2006;66:9445-52.
7. Yu YY, Ji J, Lu Y, et al. [High-resolution analysis of chromosome 5 and identification of candidate genes in gastric cancer]. *Zhonghua Zhong Liu Za Zhi* 2006; 28:84-7.
8. Jonsson G, Staaf J, Olsson E, et al. High-resolution genomic profiles of breast cancer cell lines assessed by tiling BAC array comparative genomic hybridization. *Genes Chromosomes Cancer* 2007;46:543-58.
9. Burrows JF, Chanduloy S, McIlhatton MA, et al. Altered expression of the septin gene, SEPT9, in ovarian neoplasia. *J Pathol* 2003;201:581-8.
10. Amir S, Wang R, Matzkin H, et al. MSF-A interacts with hypoxia-inducible factor-1 α and augments hypoxia-inducible factor transcriptional activation to affect tumorigenicity and angiogenesis. *Cancer Res* 2006;66: 856-66.
11. Arndt S, Poser I, Schubert T, et al. Cloning and functional characterization of a new Ski homolog, Fussel-18, specifically expressed in neuronal tissues. *Lab Invest* 2005;85:1330-41.
12. Ferguson CA, Tucker AS, Heikinheimo K, et al. The role of effectors of the actin signalling pathway, activin receptors IIA and IIB, and Smad2, in patterning of tooth development. *Development* 2001;128:4605-13.
13. Bond HM, Mesuraca M, Carbone E, et al. Early hematopoietic zinc finger protein (EHZF), the human homolog to mouse Evi3, is highly expressed in primitive human hematopoietic cells. *Blood* 2004;103: 2062-70.
14. Endo S, Zeng Q, Burke NA, et al. TGF- α antisense gene therapy inhibits head and neck squamous cell carcinoma growth *in vivo*. *Gene Ther* 2000;7:1906-14.
15. Le QT, Kong C, Lavori PW, et al. Expression and prognostic significance of a panel of tissue hypoxia markers in head-and-neck squamous cell carcinomas. *Int J Radiat Oncol Biol Phys* 2007;69:167-75.
16. Sanchez-Elsner T, Botella LM, Velasco B, et al. Synergistic cooperation between hypoxia and transforming growth factor- β pathways on human vascular endothelial growth factor gene expression. *J Biol Chem* 2001;276:38527-35.
17. Ehrlich M, Nelson MR, Stanssens P, et al. Quantitative high-throughput analysis of DNA methylation patterns by base-specific cleavage and mass spectrometry. *Proc Natl Acad Sci U S A* 2005;102:15785-90.
18. Saeed AI, Sharov V, White J, et al. TM4: a free, open-source system for microarray data management and analysis. *Biotechniques* 2003;34:374-8.
19. Smith LT, Lin M, Brena RM, et al. Epigenetic regulation of the tumor suppressor gene TCF21 on 6q23-24 in lung and head and neck cancer. *Proc Natl Acad Sci U S A* 2006;103:982-7.
20. St John MA, Abemayor E, Wong DT. Recent new approaches to the treatment of head and neck cancer. *Anticancer Drugs* 2006;17:365-75.